eLIFE elifesciences.org

RESEARCH ARTICLE

Figures and figure supplements

Bladder-cancer-associated mutations in *RXRA* activate peroxisome proliferator-activated receptors to drive urothelial proliferation

Angela M Halstead *et al*

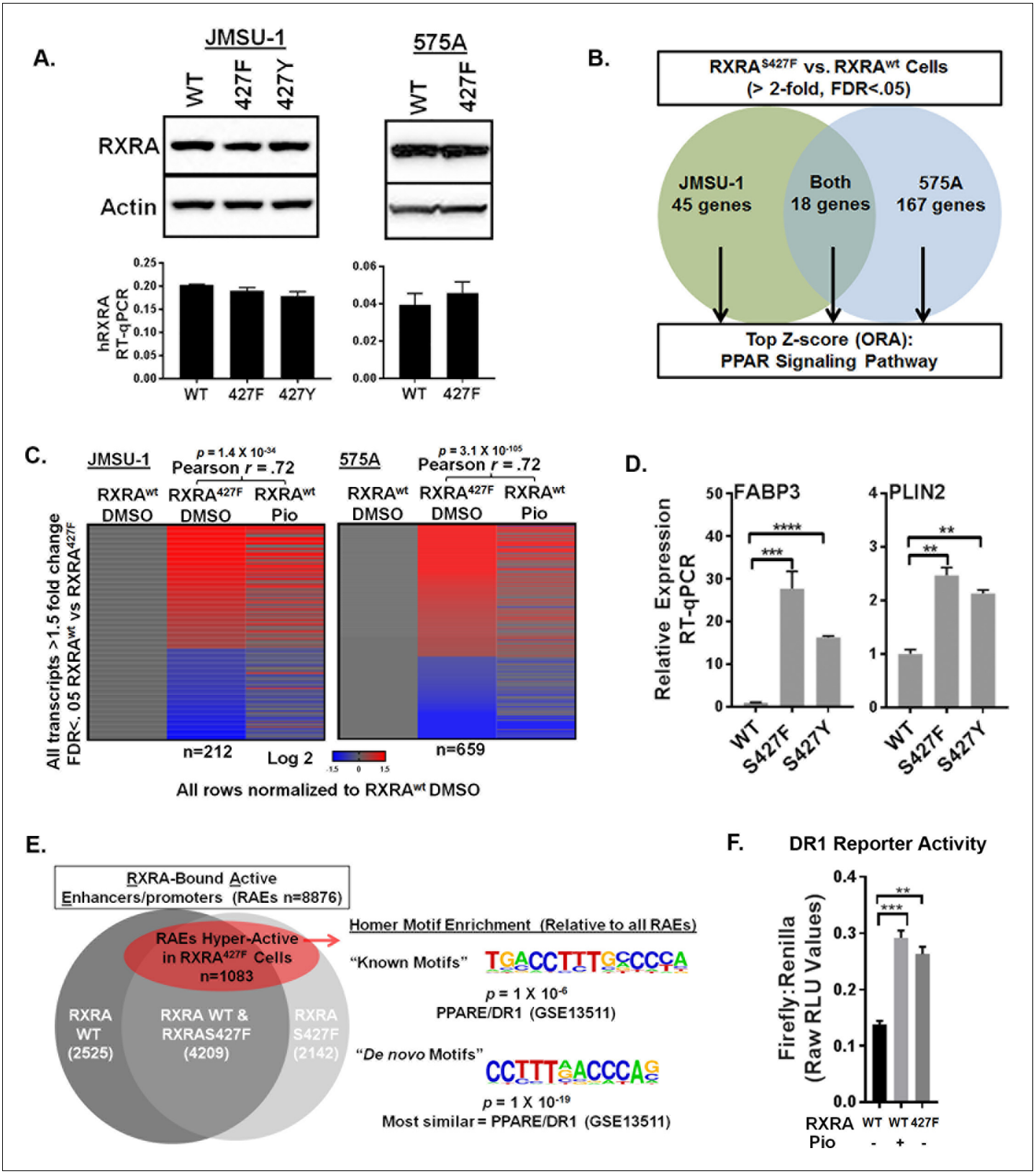

Figure 1. RXRA hot-spot mutations induce the PPAR signaling pathway by activating enhancer/promoters with a canonical PPAR response element. (**A**) JMSU-1 and 575A cells were transduced with pBABE retrovirus to express indicated RXRA alleles and expression confirmed by western blot (top) or RT-qPCR in triplicate ± SD (data expressed as a fraction of actin signal). (**B**) Protein coding transcripts up-regulated greater than or equal to twofold

Figure 1 continued on next page

Figure 1 continued

(FDR < 0.05) in cells expressing $RXRA^{S427F}$ compared to cells expressing $RXRA^{wt}$ were identified and then subjected to over representation analysis (ORA, GO-Elite) to discover enriched pathways relative to all other protein coding transcripts identified by RNA-seq. Experiment was done in two bladder cancer cell lines, JMSU-1 or 575A, using three RNA samples, each purified from an independent cell well, for each condition. (See also source data 1). (**C**) Transcriptome changes induced by $RXRA^{S427F}$ relative to $RXRA^{wt}$ were compared to expression changes of the same transcripts induced by 16 hr of pioglitazone (1 μM) treatment in the $RXRA^{wt}$ expressing cells. **D**) Relative expression of two PPAR targets with expression of indicated *RXRA* alleles. RT-qPCR performed in triplicate ±SD. Comparison by Student's t-test. (**E**) RAEs were defined by the presence of overlapping ChIP-seq signal for RXRA and H3K27ac. RAEs identified by binding of $RXRA^{wt}$ and/or $RXRA^{S427F}$ are represented in grey. Hyperactive RAEs represented in red had elevated H3K27ac mean peak height in the mutant expressing cells compared to the wild-type cells (FDR < 0.05). All ChIP-seq peak callings were based on data from three independent immuno-precipitations, each utilizing input material from an independent cell plate. HOMER motif analysis was used to identify motifs enriched in hyperactive RAEs relative to the background of non-hyperactive RAEs. Source data 2 specifies number of peaks in each sector of the venn diagram. (**F**) Activity of a DR1 response element reporter (3X PPRE) transfected into JMSU-1 cells stably expressing either $RXRA^{wt}$ or $RXRA^{S427F}$. $RXRA^{wt}$ cells were also treated with pioglitazone (1 μM) for 16 hr. For all reporter assays, Firefly luciferase expressing reporter was co-transfected with a constitutive Renilla luciferase expression vector to normalize for transfection efficiency. Data represents mean ± SEM of Firefly to Renilla luciferase signal from three independent experiments done on different days, each performed using triplicate cell wells. Statistical comparisons are by paired *t*-test.

DOI: https://doi.org/10.7554/eLife.30862.003

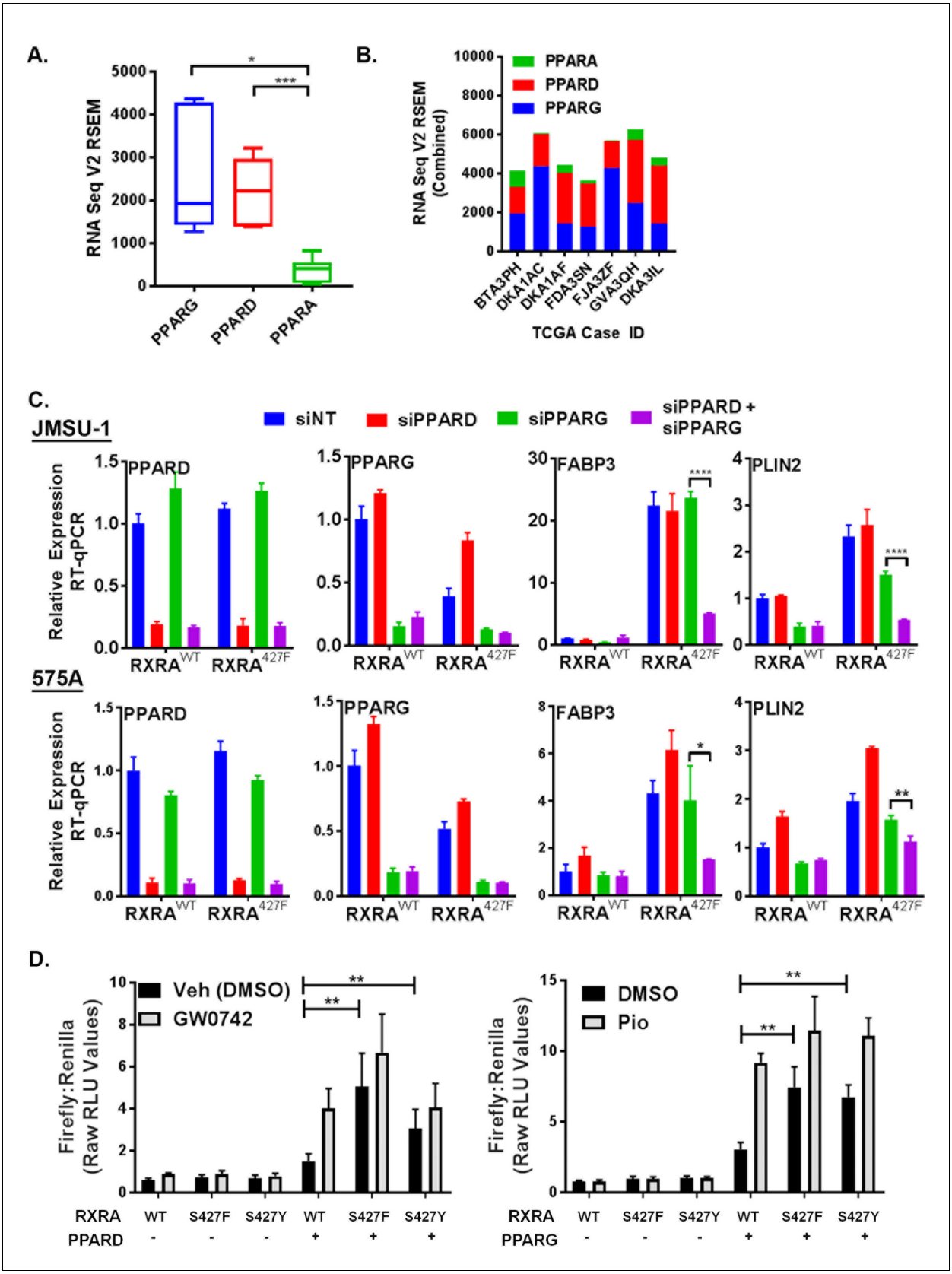

Figure 2. PPARG or PPARD expression is necessary and sufficient for mutant RXRA activity. **A**) PPAR RNA expression in RXRA hot-spot mutant clinical samples from the TCGA dataset. Whisker plot shows 25th, median, and 75th percentile. (**B**) Data from panel A plotted per patient with hot-spot

Figure 2 continued on next page

Figure 2 continued

mutation. (**C**) Effects of siRNA-mediated knock-down of *PPARD* and *PPARG* in JMSU-1 and 575A cell lines on two target genes (*PLIN2* and *FABP3*) up-regulated by mutant RXRA. Data by RT-qPCR in triplicate ±SD and indicated comparisons by Student's t-test. (**D**) DR1 luciferase reporter activity in UM-UC-3 cells transfected with RXRA ±PPARD or PPARG. Cells were treated with 1 μM of the PPARG agonist pioglitazone or the PPARD agonist GW0742 for 16 hr. Data represents mean ±SEM of Firefly to Renilla luciferase signal from three independent experiments done on different days, each performed using triplicate cell wells. Statistical comparisons are by paired *t*-test.

DOI: https://doi.org/10.7554/eLife.30862.006

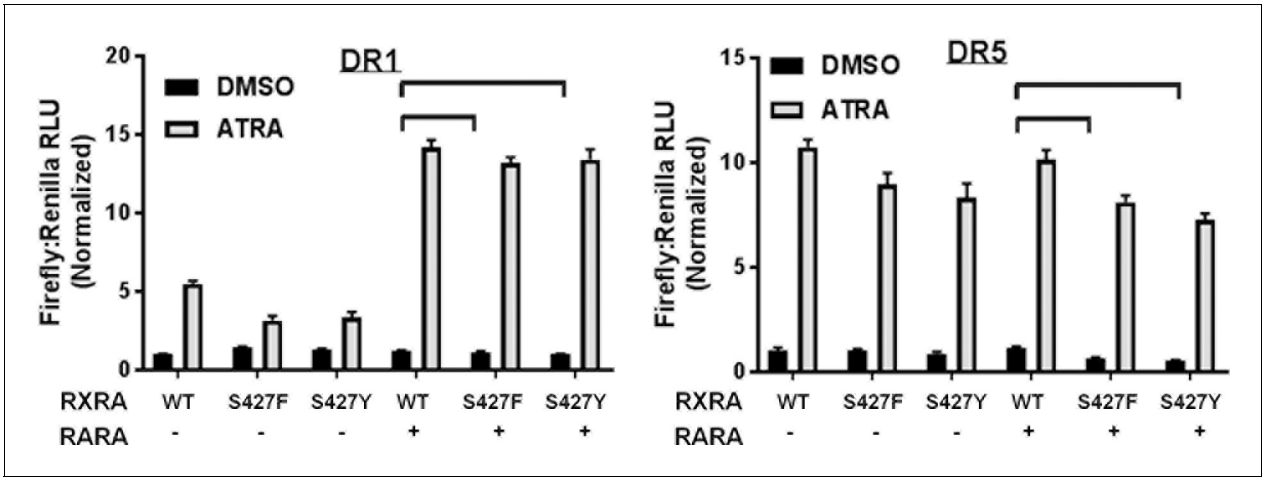

Figure 2—figure supplement 1. RARA expression is not sufficient for mutant RXRA hyperactivity. (**A**) DR1 and DR5 luciferase reporter activity in UM-UC-3 cells transfected with RXRA ±RARA as indicated and treated with 100 nM all-trans-retinoic acid (ATRA) for 16 hr.
DOI: https://doi.org/10.7554/eLife.30862.007

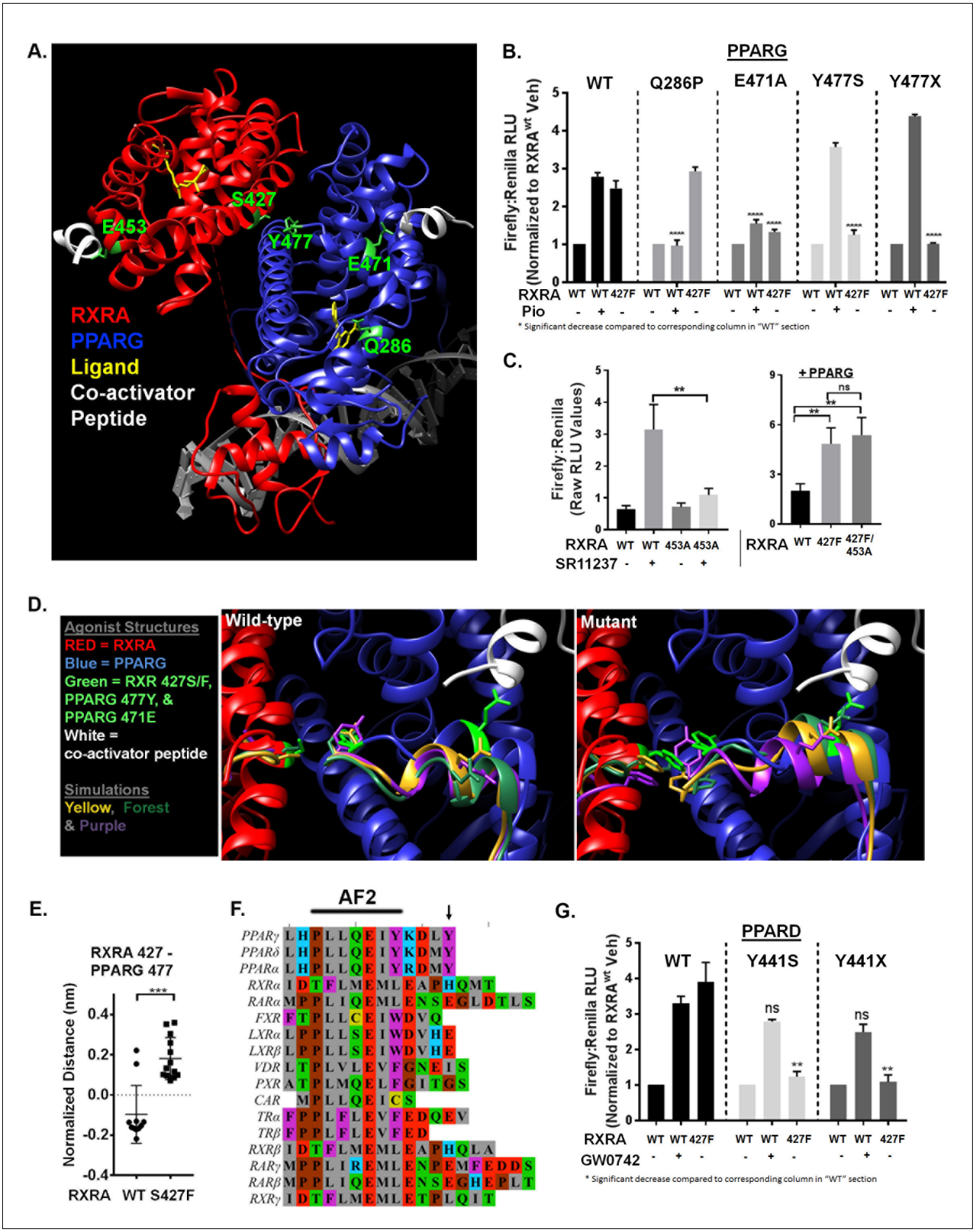

Figure 3. Mutant RXRA induces allosteric activation of PPARs through their terminal tyrosine. **A**) RXRA S427 and other amino acids mutated for structure-function studies highlighted in green on a published full-length crystal structure of a RXRA/PPARG heterodimer. (**B**) DR1 reporter assay in UM-

Figure 3 continued on next page

Figure 3 continued

UC-3 co-transfecting indicated RXRA and PPARG alleles. Cells were treated with vehicle (DMSO) or pioglitazone 1 μM for 16 hr. Data represents mean normalized signal ±SEM of three independent experiments done on different days, each performed in triplicate, with data from each experiment normalized to the $RXRA^{wt}$ vehicle condition for each section. Statistical comparisons are by unpaired *t*-test. (**C**) Left, reporter assay performed with indicated RXRA alleles only and drug treatment with the RXRA agonist SR11237 (100 nM) for 16 hr. Right, reporter assay with wild-type PPARG co-transfected. Data represent mean ±SEM of Firefly to Renilla luciferase signal from three independent experiments done on different days, each performed using triplicate cell wells. Statistical comparisons are by paired *t*-test. (**D**) Published agonist structure of RXRA/PPARG heterodimer (PDB: 1FM6) in red and blue with key residues highlighted in bright green. Top three occupied microstate clusters from simulation experiments are superimposed. (**E**) Distance from starting agonist structure between alpha carbons of RXR 427 and PPARG 477 in the top 5% most-occupied microstates for wild-type and mutant RXRA. Mean ±SD, comparison is by Student's t test. (**F**) Alignment of the AF2 region and C-terminus of all RXRA dimerization partners. Terminal tyrosine unique to PPARs is indicated. (**G**) Reporter assay similar to B, but using PPARD and the PPARD agonist GW0742.

DOI: https://doi.org/10.7554/eLife.30862.008

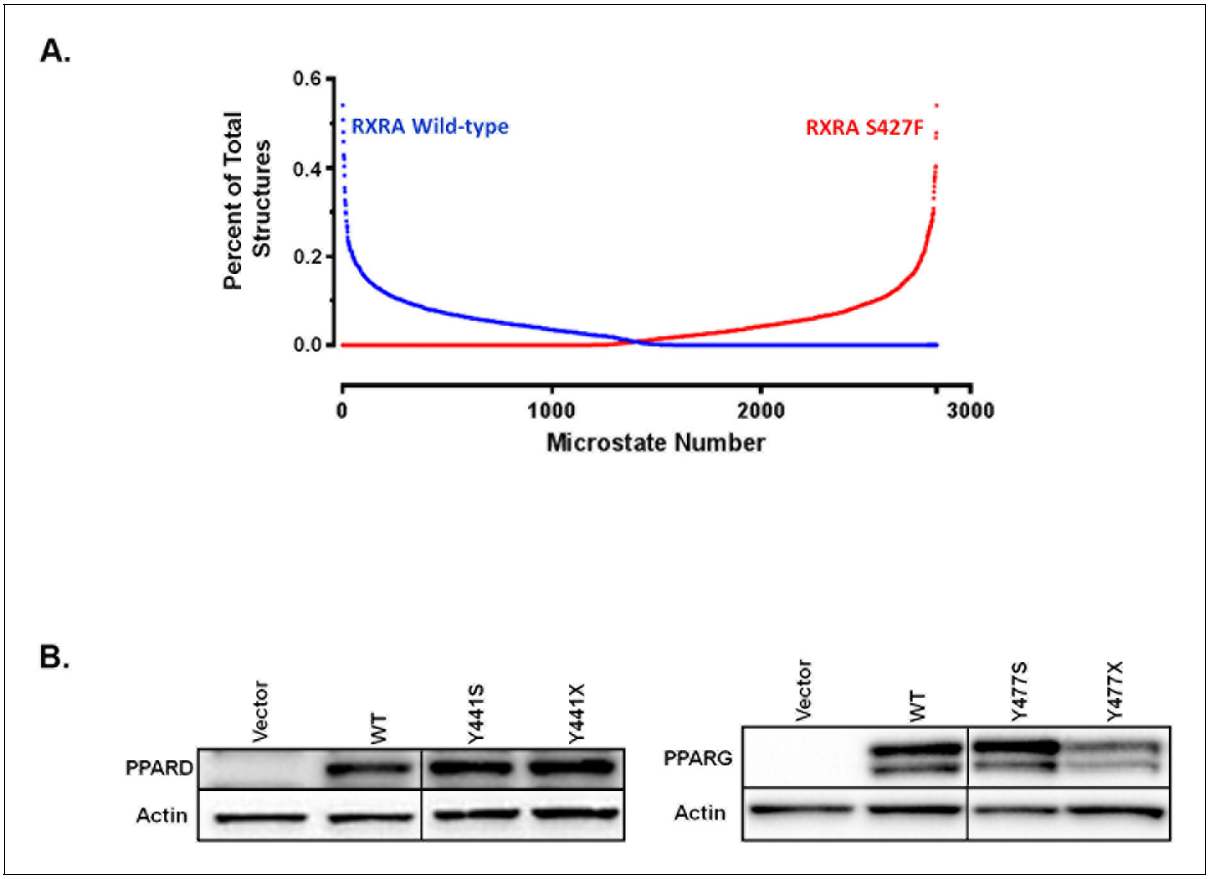

Figure 3—figure supplement 1. (**A**) Distribution of micro-state clusters occupied in $RXRA^{wt}$ and $RXRA^{S427F}$ simulations. (**B**) Western blot confirming expression of PPARD and PPARG with terminal tyrosine mutation or deletion in transfected UM-UC-3 cells. Irrelevant intervening lanes were removed where indicated with vertical bar without further image manipulation.

DOI: https://doi.org/10.7554/eLife.30862.009

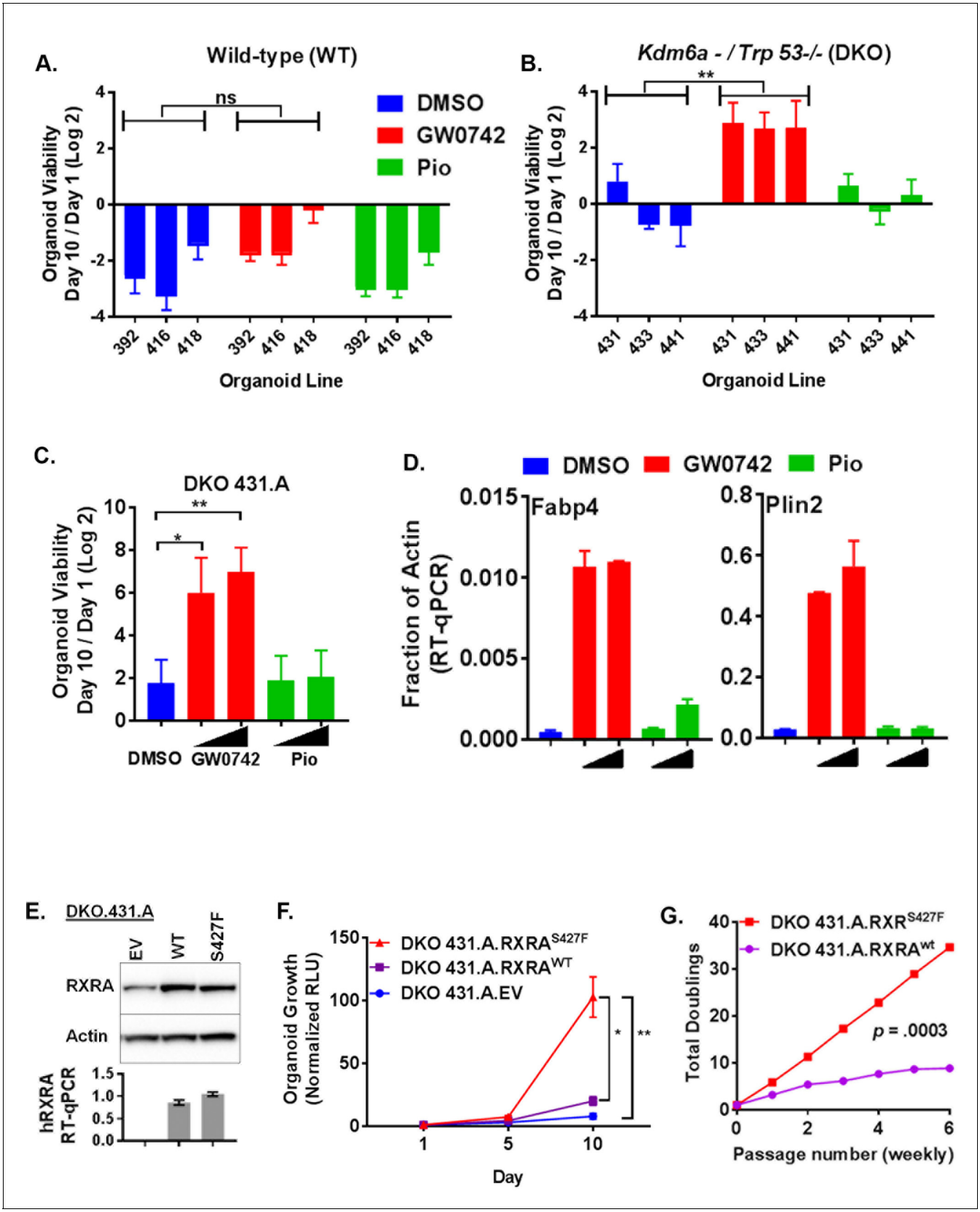

Figure 4. PPARD agonist and mutant RXRA confer growth-factor-independent growth to urothelium in the context of tumor suppressor loss. (**A**) Organoids were derived from three independent wild-type mouse bladders and infected with Adeno-Cre. Growth was determined for each line in

Figure 4 continued on next page

Figure 4 continued

organoid media without EGF using CellTiter-Glo after treatment with vehicle, GW0742 (100 nM), or pioglitazone (100 nM). Data represent mean ±SEM from three independent experiments, each performed in triplicate cell wells. Statistical comparison is by unpaired *t*-test. (**B**) Similar to A but organoids were derived from $Trp53^{flox/flox}$; $Kdm6a^{flox}$ mice. (**C**) CellTiter-Glo growth assay in media without EGF of a sub-clone from DKO431 (DKO 431.A) treated with GW0742 (10, 100 nM) or pioglitazone (100, 1000 nM). Mean values ± SEM from three independent experiments, each performed using triplicate organoid wells. Comparison is by paired *t*-test. (**D**) DKO 431.A organoids were plated in standard organoid media and then treated with, vehicle, GW0742 (10, 100 nM)) or pioglitazone (100, 1000 nM) for an additional 48 hr. Induction of PPAR target genes was determined by RT-qPCR in triplicate ± SD. (See also ***Figure 4—figure supplement 1C***.) (**E**) DKO 431.A organoids were infected with a retroviral vector that was empty, expresses $RXRA^{wt}$, or expresses $RXRA^{S427F}$ and expression of total RXRA (western blot) and human *RXRA* (RT-qPCR, triplicate +/SD) was determined. (**F**) Mean CellTiter-Glo signal ±SEM from three identical experiments, each performed using triplicate organoid wells. Comparison of D10 data is by paired *t*-test. (**G**) Identical number of indicated organoid cells were plated in media without EGF and then harvested with trypsin weekly and counted in duplicate using a BioRad TC20. Identical numbers of cells were then re-plated and this was repeated for 6 weeks. Total cell number doublings were calculated and plotted. Comparison of doublings is by paired *t*-test.

DOI: https://doi.org/10.7554/eLife.30862.010

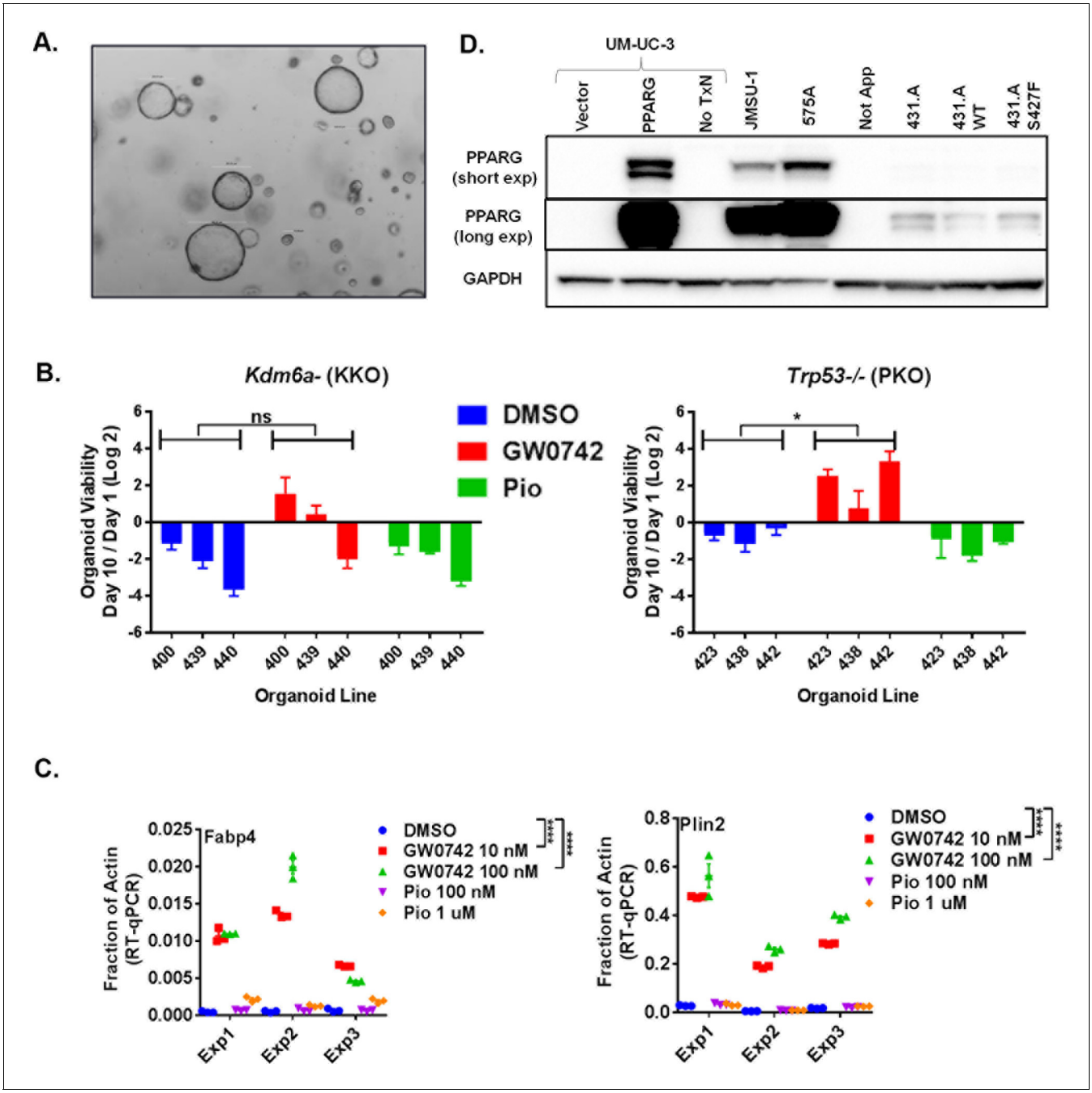

Figure 4—figure supplement 1. (**A**) Wild-type urothelial organoids grown for 3 weeks in standard organoid media and imaged with low-power (4X) phase contrast bright-field microscopy. (**B**) CellTiter-glo growth assay in media without EGF performed identically to those in ***Figure 4A*** and ***Figure 4B***, but with organoids generated from mice with singly floxed *Trp53* or *Kdm6a*. Statistical comparisons are by unpaired *t* test. (**C**) Aggregated RT-qPCR from three distinct experiments as described in ***Figure 4D*** with each data point from each experiment plotted with mean indicated. Statistical comparisons are by two-way ANOVA (Repeated Measures, GraphPad Prism). (**D**) PPARG western blot of indicated cell lines. PPARG transfected UM-UC-3 included as a positive control. Equivalent protein mass from whole cell lysates were loaded into each well.

DOI: https://doi.org/10.7554/eLife.30862.011

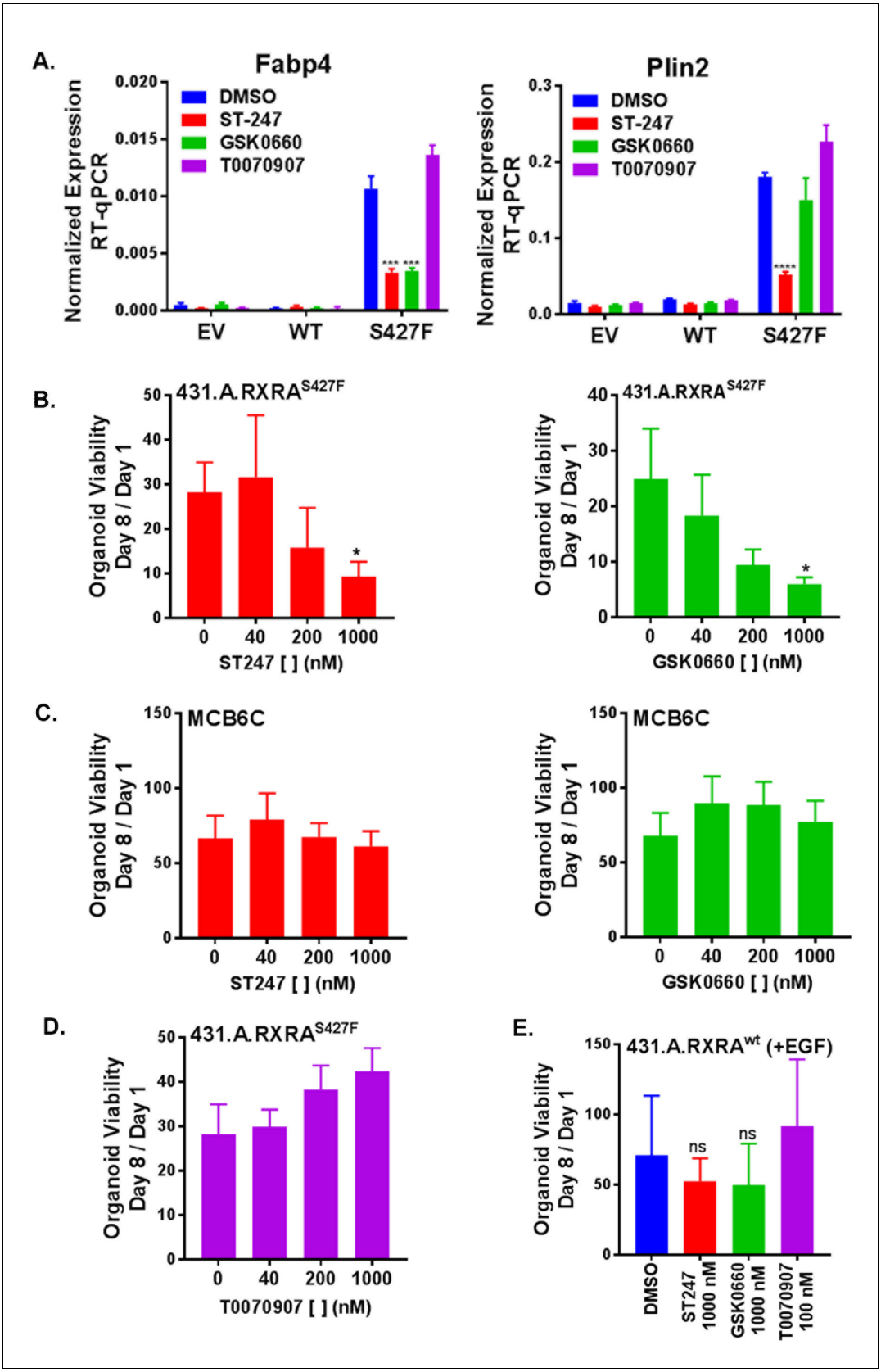

Figure 5. RXRA S427F generates PPARD-dependent urothelial growth. (**A**) Retrovirally transduced organoids from ***Figure 4*** were plated for 7 days in standard media and then treated with the indicated PPARD antagonists (1000 nM ST-247, GSK0660) or PPARG antagonist (100 nM T0070907) for 2 days.

Figure 5 continued on next page

Figure 5 continued

Expression of PPAR targets was determined by RT-qPCR in triplicate ±SD and comparison is by Student's t-test to the $RXRA^{S427F}$ DMSO condition. (See also ***Figure 5—figure supplement 1***)) (**B-E**) CellTiter-Glo growth assay of indicated organoid lines treated with indicated drugs. Plotted is mean signal ±SEM from three independent experiments, each performed using triplicate organoid wells. MCB6C is an organoid line we derived from a carcinogen-induced bladder tumor and lacks RXRA mutation. Organoids were cultured in media without EGF except for panel E where inclusion of EGF is indicated. Comparison is to DMSO condition using paired *t*-test.

DOI: https://doi.org/10.7554/eLife.30862.012

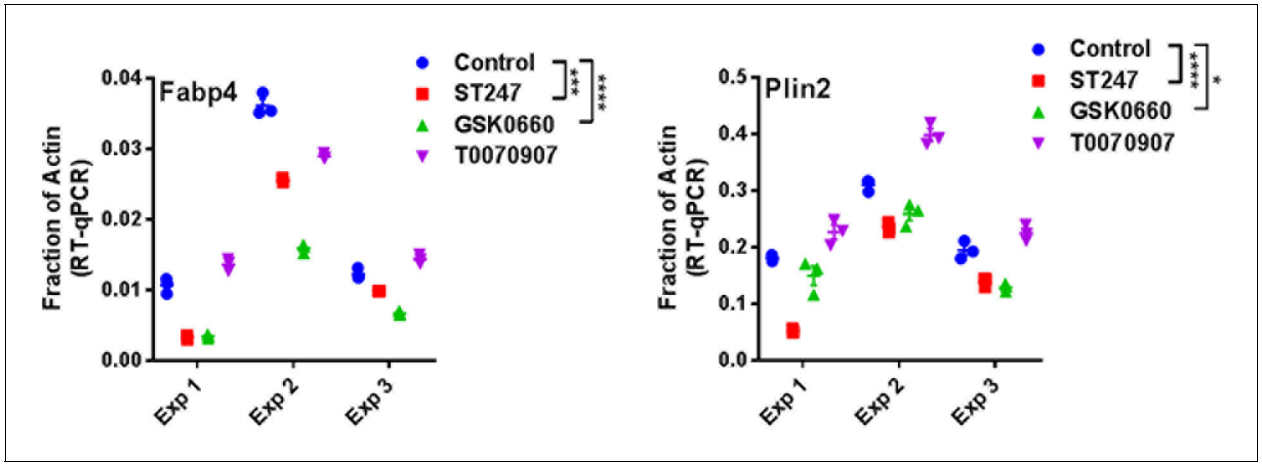

Figure 5—figure supplement 1. Aggregated RT-qPCR from three distinct experiments as described in ***Figure 5A*** with each data point from each experiment plotted with mean indicated. Statistical comparisons are by two-way ANOVA (repeated measures, GraphPad Prism).

DOI: https://doi.org/10.7554/eLife.30862.013